Cancer Chemother Pharmacol (2008) 62:595–604
DOI 10.1007/s00280-007-0643-0

ORIGINAL ARTICLE

Biological properties of 4-methyl-2,7-diamino-5,10-diphenyl-4,9-diazapyrenium hydrogensulfate (ADAP)

Saška Marczi · Ljubica Glavaš-Obrovac · Tatjana Belovari · Ranko Stojković · Siniša Ivanković · Vatroslav Šerić · Ivo Piantanida · Mladen Žinić

Received: 11 September 2007 / Accepted: 31 October 2007 / Published online: 23 November 2007

Abstract
Objective 4-Methyl-2,7-diamino-5,10-diphenyl-4,9-diazapyrenium hydrogensulfate (ADAP) is a potential antitumor compound because of its DNA and RNA intercalating ability. In this study, cellular uptake, intracellular distribution as well as mechanism of action, antitumor activity in vitro and toxicity in vivo of ADAP were investigated.
Methods Based on the fluorescence properties of ADAP, its entry and distribution into live cells were analyzed by fluorescence microscopy. The in vitro antiproliferative activity was determined using MTT test. For screening of topoisomerase II-targeted effects of ADAP, the cell-free assay and immunoband depletion assay were used. Expression of the genes *c-mos*, *c-N-ras*, *c-Ki-ras*, *c-H-ras*, *p53* and *caspase 3* in Caco-2 cells treated with ADAP was examined by RT-PCR. Toxicity in vivo was determined using C3HHf/Bu Zgr/Hr mice treated by single or multiple doses of ADAP at a concentration of 25 mg/kg.
Results ADAP in μM concentrations entered into MIAPaCa-2 cell's cytoplasm in 5 min and into nuclei in 60 min after administration. Intracellular distribution of ADAP depended on the period of treatment time. ADAP (0.1–100 μM) strongly inhibited the growth of both mouse (FsaR, SCCVII) and human tumor cells (HeLa, Caco-2, HT-29, MIAPaCa-2, HBL, HEp-2, SW620, MCF-7) compared to its weak cytotoxicity on controls and normal cells (WI38). Results of both topoisomerase II assays showed that ADAP is not a topoisomerase II poison. Expression of investigated genes was dependent on the incubation time, except for *p53* and *c-H-ras*. Morphological changes in tissues and organs of mice were not observed. Results of patohistological analysis have been confirmed by hematological and clinical-chemical analysis of blood of treated and non-treated animals.
Conclusion ADAP is a strongly bioactive compound with antitumor potential in vitro. The antitumor potential in vivo remains to be identified.

Keywords 4,9-Diazapyrenium derivatives · Cellular uptake · Intracellular distribution · Cytotoxicity in vitro · Topoisomerase IIα · Mice · Toxicity in vivo

S. Marczi · L. Glavaš-Obrovac
Department of Nuclear Medicine and Pathophysiology, Clinical Hospital Osijek, Osijek, Croatia

L. Glavaš-Obrovac (✉)
Department of Chemistry, Biochemistry and Clinical Chemistry, School of Medicine Osijek, Huttlerova 4, 31000 Osijek, Croatia
e-mail: glavas-obrovac.ljubica@kbo.hr

T. Belovari
Department of Histology and Embriology, School of Medicine Osijek, Osijek, Croatia

R. Stojković · S. Ivanković
Division of Molecular Medicine, Ruđer Bošković Institute, Zagreb, Croatia

V. Šerić
Department of Clinical Biochemistry, Clinical Hospital Osijek, Osijek, Croatia

I. Piantanida · M. Žinić
Division of Organic Chemistry and Biochemistry, Ruđer Bošković Institute, Zagreb, Croatia

Introduction

Cancer is not a single disease but a wide group of neoplasm with diverse genetic abnormalities and variable responses

to treatment. High prevalence, high death rate, and ineffective therapy have spurred the search for novel strategies in the treatment of cancer [1–3]. Organic molecules, which interact with DNA, RNA and/or proteins, have the potential to inhibit the activity of structurally and functionally important molecules in the tumor cells. Since 1960s, when Lerman [4] introduced the DNA intercalation concept, numerous intercalators have been developed. This mode of binding is characterized by low selectivity towards different DNA and RNA sequences as well as low or non-selective bioactivity [5]. However, the activity of many antitumor drugs is based on intercalation but selectivity could be improved by introduction of specific subtituents on the intercalative aromatic core [6]. DNA intercalators are important drugs for cancer therapy today. Some of the DNA intercalators such as doxorubicin, epirubicin, mitoxantrone and *m*-AMSA are currently used in treatment of different carcinomas and leukemias, and the others are in a broad use as nucleic acid dyes [7–9]. Several antibiotics are DNA intercalators and are recognized as the new, promising class of DNA antitumor agents [10]. Numerous intercalating compounds are currently in various stages of preclinical and clinical evaluation [11, 12]. However, the search for new intercalators with cytotoxic feature and the capability to overcome many barriers in live organism to reach the target structure in the cells and with as little as possible side effects is necessary.

DNA intercalators can act as inhibitors of enzymes which assemble on DNA molecules during the cellular DNA processes like DNA replication, transcription, recombination, formation of nucleosomes and DNA repair. Topoisomerase II, an essential enzyme that participates in all DNA processes, interconverts the topology of DNA by making a transient double stranded break and passing the segment of DNA through it. The transient covalent bond between the DNA ends of double stranded break and topoisomerase II is called "cleavage" complex. Some of the most successful anticancer compounds stabilize the "cleavage" complex by converting the topoisomerase II into cellular toxin. These drugs, named as topoisomerase II poisons, include some of the DNA intercalators (epirubicin, doxorubicin, idarubicin, daunorubicin, mitoxantron, *m*-AMSA) among the drugs with different mechanism of action (etoposide, teniposide) [13]. The result of their action is accumulation of stabilized, irreversible "cleavage" complexes, i.e. DNA breaks that can trigger the apoptosis [14–17].

4-Methyl-2,7-diamino-5,10-diphenyl-4,9-diazapyrenium hydrogensulfate (ADAP) is a molecule belonging to the 4,9-diazapyrenium compound and a known nucleic acids intercalator [18–21]. The fluorescence properties of ADAP are highly sensitive to basepair composition of polynucleotides. The ADAP's strong fluorescence in the red part of the visible spectrum (λ = 615 nm) allows the monitoring of the ADAPs uptake and intracellular distribution in live cells by fluorescence microscopy. ADAP has been developed as a potential antitumor compound with higher stability in comparison to other related 4,9-diazapyrenium compounds whose biological activity is already analyzed [22–25]. The new features of ADAP, in comparison to other 4,9-diazapyrenium compounds, are two amino groups positioned on the opposite sides of longer axis of the molecule, which can form additional interactions with double- and single- stranded DNA and RNA and induce selectivity [20].

Materials and methods

Chemicals

ADAP was synthesized at the Laboratory for Supramolecular and Nucleoside Chemistry, Department of Chemistry and Biochemistry, Ruđer Bošković Institute, Zagreb, Croatia (Fig. 1). For biological assays, ADAP was dissolved and diluted in distilled water immediately before use. 4′,6-Diamidine-2′-phenylindole dihydrochloride (DAPI) was obtained from Roche-Boehringer (Mannheim, Germany). Propidium iodide (PI) was obtained from Molecular Probes, Invitrogen (Paisley, UK). Working solution of PI (0.01 μM) was made in distilled water immediately before use. 4-[9-Acridinylamino]-*N*-[methanesulfonyl])-*m*-anisidide (*m*-AMSA) was obtained from Sigma Biochemicals (St Louis, USA).

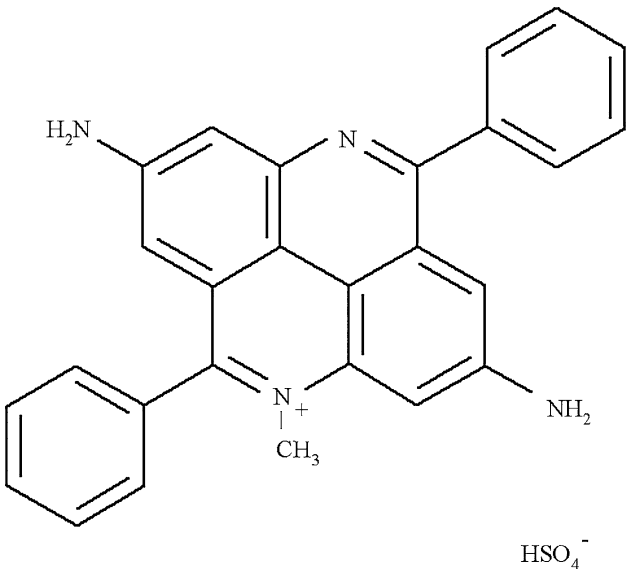

Fig. 1 Chemical structure of 4-methyl-2,7-diamino-5,10-diphenyl-4,9-diazpyrenium hydrogensulfate (ADAP)

Uptake and intracellular distribution of ADAP

MIAPaCa-2 cells, selected due to their extended morphology, were grown on microscopic slides (1×10^5 cells/slide) at 37°C for 24 h. Three groups of tests were performed: (1) Cells were incubated with ADAP (0.1 and 1 μM, in DME medium) for 5 and 60 min, then washed with PBS and incubated in DAPI-methanol working solution (1 nM) for 5 min at room temperature in the dark. DAPI-methanol working solution was poured off, cells were rinsed with PBS, covered and analyzed. (2) Cells were incubated with ADAP (10 μM, in DME medium) for 60 and 120 min, rinsed with PBS, covered with a glass coverslip and analyzed. (3) Control cells, in order to confirm the cells viability, were treated in PI solution (0.01 μM) for 5 min, washed with PBS and analyzed under the microscope (PBS as mounting medium). The entry and intracellular distribution of tested chemicals were analyzed under the fluorescence microscope (Axioskop 2 MOT, Carl Zeiss Jena GmbH, Jena, Germany) with Zeiss filter combinations: (f1) BP 365/12, FT 395, LP 397, (f2) BP 530–585, FT 600, LP 615 and (f3) BP 450–490, LP 520.

Cell cultures and in vitro cytotoxicity determination

Human cell lines: normal fibroblasts (WI38), melanoma (HBL), larynx carcinoma (HEp-2), cervical carcinoma (HeLa), colon carcinoma (Caco-2 and HT-29), poorly differentiated cells from lymph node metastasis of colon carcinoma (SW620), breast carcinoma (MCF-7), pancreatic carcinoma (MIAPaCa-2), and mouse cell lines: fibrosarcoma (FsaR) and squamous carcinoma (SCCVII) were used in antiproliferation investigation experiments. Cells were grown as a monolayer at 37°C in a humidified atmosphere with 5% CO_2. Human cell lines were cultivated in DME medium (Institute of Immunology Inc., Zagreb, Croatia) supplemented with 10% FBS (Gibco BRL, Life Technologies, Paisley, UK) and 2 mM L-glutamine (Sigma Biochemicals, St Louis, USA). Mouse cell lines were cultivated in RPMI medium (Institute of Immunology Inc., Zagreb, Croatia) supplemented with 10% FBS and 2 mM L-glutamine. Growth inhibition effects of ADAP were determined using MTT assay [26]. Human and mouse cells in exponential growth phase, 2×10^4 cells per mL, were plated onto 96-microwell plates. Twenty-four hours later, cells were exposed to different concentrations of ADAP (100 – 0.1 μM). At the end of 72 h treatment, medium was removed and 40 μL of 3-(4,5-dimethyl-2-thiazolyl)-2,5-diphenyl-2H-tetrazolium bromide (MTT) (Merck, Darmstadt, Germany), diluted in PBS, was added to each well and incubated for another 4 h. The optical density was read on the ELISA reader StatFax 2100 microplate reader at 570 nm, after the formazan was dissolved in DMSO. All experiments were performed at least three times, with three wells for each concentration of ADAP. The control cells were grown under the same conditions without addition of the tested compound. The inhibitory rate was calculated as follows:

$$\text{Inhibitory rate}\% = \text{absorption}_{\text{control}} - \text{absorption}_{\text{test}} / \text{absorption}_{\text{control}} \times 100$$

Screening of topoisomerase II-targeted effects

Cell-free assay

Inhibition of human topoisomerase IIα activity was performed following the procedure of Burden et al. [27]. Supercoiled pBR322 plasmid DNA (290 ng) (Sigma Biochemicals, St Louis, USA) was incubated with reaction buffer (10 mM Tris–HCl, pH 7.9, 50 mM NaCl, 50 mM KCl, 0.1 mM Na_2EDTA, 5 mM $MgCl_2$, 2.5% glycerol) and 10 U of human topoisomerase IIα (Sigma Biochemicals, St Louis, USA) in the absence or presence of ADAP, or *m*-AMSA, in final volume of 20 μl. Incubation at 37°C for 15 min was terminated by addition of 10% SDS and 250 mM Na_2EDTA. Samples were then digested with 0.8 g/L proteinase K at 60°C for 30 min. The control was pBR322 DNA without drugs and enzymes. Linearized pBR322 DNA was obtained by digestion of plasmid DNA with an 80 U *Hin*dIII restriction enzyme (Amersham Pharmacia Biotech, Little Chalfont, UK) at 37°C for 60 min. Nicked pBR322 DNA was obtained by digestion with 0.02 U DNaseI (Amersham Pharmacia Biotech, Little Chalfont, UK) at 37°C for 10 min. Gel electrophoresis was performed in 1% agarose gels with 1× TAE buffer. The gel was stained for 30 min in a solution of 1 mg/L ethidium bromide in 1× TAE buffer following electrophoresis. DNA bands were visualized by UV-transiluminator (Pharmacia, Sweden).

Immunoband depletion assay

Immunoband depletion assay has been performed as described by Kaufmann and Svingen [28]. After the Caco-2 cells were washed with serum-free medium, detached by trypsin/EDTA and its concentration adjusted to 2×10^6 cells per 1 ml serum-free medium, samples were incubated with ADAP (100 μM), or control compound *m*-AMSA (100 μM), for 45 min at 37°C. Cells were centrifuged at 1,100 rpm for 5 min and lysed (0.25% SDS, 10 mM $MgCl_2$, 50 mM Tris–HCl, pH 7.4, 200 μg/ml EDTA, 2 mM PMSF) on ice for 60 min. Lysate proteins were separated by 12.5% SDS-PAGE as described by Laemmli [29] and transferred to PVDF membranes (Bio-Rad Laboratories, Hercules, USA). The blots were incubated in

blocking solution consisting of 3% BSA and 0.05% Tween-20 in PBS pH 7.2 for 60 min. The topoisomerase IIα bands were visualized using mouse monoclonal IgG against human topoisomerase IIα (Dako, Glostrup, Denmark), horseradish peroxidase conjugated goat anti-mouse IgG (Santa Cruz Biotechnology, Santa Cruz, USA), diaminbenzidine and H_2O_2. Relative quantification of topoisomerase IIα bands was performed using ImageQuant^{TL} software (GE Healthcare, Vienna, Austria) and normalized to control bands (untreated cells).

RT-PCR

Total RNA of Caco-2 cells treated with 1 μM ADAP during 3, 12 and 24 h was extracted using the "QuickPrep^{TM} Total RNA Extraction Kit" (Amersham Pharmacia Biotech, Little Chalfont, UK) according to the manufacturer's instructions. A weight of 0.25 μg of total RNA was used as a template in a reverse transcription reaction containing 200 U SuperScript^{TM} reverse transcriptase (Invitrogen, Paisley, UK), 0.025 μg/ml $p(dT)_{15}$ primers (Roche Diagnostics, Mannheim, Germany), 0.5 mM dNTPs each (Roche Diagnostics, Mannheim, Germany) and 10 mM DTT in a 20 μl final volume. The PCR was performed in a final volume of 50 μl containing 2 mM $MgCl_2$, 0.2 mM of each dNTP, 4 U Taq DNA polymerase (Invitrogen, Paisley, UK) and 0.5 μM of primer. The amplification primers used were: *GAPDH* 5′-CCA TCA ATG ACC CCT TCA TTG ACC-3′ sense, 5′-GAA GGC CAT GCC AGT GAG CTT CC-3′ antisense; *p53* 5′-GAT GCT GTC CGC GGA CGA TAT-3′ sense, 5′-CGT GCA AGT CAC AGA CTT GGC-3′ antisense; *caspase 3* 5′-TCG GTC TGG TAC AGA TGT CG-3′ sense, 5′-CAT ACA AGA AGT CGG CCT CC-3′ antisense; *c-Ki-ras* 5′-TTC CTA CAG GAA GCA AGT AG-3′ sense, 5′-CAC AAA GAA AGC CCT CCC CA-3′ antisense; *c-H-ras* 5′-GAC GGA ATA TAA GCT GGT GG-3′ sense, 5′-AGG CAC GTC TCC CCA TCA AT-3′ antisense; *c-N-ras* 5′-GGT GAA ACC TGT TTG TTG GA-3′ sense, 5′-ATA CAC AGA GGA AGC CTT CG-3′ antisense and *c-mos* 5′-GCA GCA GTC CCT CAG AGC TA-3′ sense, 5′-CGC CAT AGA TGA CTT GGT GT-3′ antisense. After an initial denaturation step at 95°C for 2.5 min, 35 cycles were performed with each cycle consisting of denaturation at 95°C for 30 s, annealing of the primers (*GAPDH* at 68°C, *p53* at 61°C, *c-Ki-ras* at 57°C and 53°C, *c-H-ras* at 56°C, *c-N-ras* at 54°C and *c-mos* at 59°C and 55°C) for 1.5 min and elongation at 72°C for 1 min. Two-step RT-PCR was carried out on the Progene Thermal Cycler (Techne Cambridge Ltd., UK). The RT-PCR amplification products (an 5 μl aliquot) were subjected to electrophoresis in a 2% agarose gel stained with ethidium bromide. The intensity of the bends was analyzed using ImageQuant^{TL} software and normalized to intensity of the control bands.

Determination of toxicity in vivo

Experimental Animals

C3HHf/Bu Zgr/Hr male mice were used. Animals were 14–16 weeks old and weighed 23–26 g at the time of treatment. Six mice were used in each group per experiment. Each experiment was repeated twice. Mice were obtained from Rudjer Boskovic Institute's breeding colony. During the experimental period, three animals were kept per cage. Bottom of the cage was covered with sawdust (Allspan®, Germany). Standard food for laboratory mice (4 RF 21 GLP Mmucedola srl, Italy) was used. All animals had access to food and water ad libitum. Animals were kept in conventional circumstances: light/dark rhythms 12/12 h, temperature 22°C, and humidity 55%. All experiments were performed according to the ILAR Guide for the Care and Use of Laboratory Animals, Council Directive (86/609/EEC) and Croatian animal welfare law (NN 19/99).

Test compound and dosage

ADAP was stored at +4°C and freshly dissolved in distilled water immediately prior to injection (for each application). According to results of IC_{50} values of in vitro cytotoxicity and results of in vivo acute toxicity investigations (data not shown), a dose of 25 mg/kg was used to study the toxic effects of ADAP. The drug was administered through intraperitoneal (i.p.) route as a single dose of 25 mg/kg or multiple applications (day 1, 3, 5, 7, 9) of the same dose (total dose 125 mg/kg). On 7th or 21st day after treatment, animals were anesthetized by carbon dioxide, killed and blood was collected for hematological and clinical-chemical analysis. Organs (liver, kidney, lung, spleen, heart, testicle, stomach, brain, bone, small intestine, colon, and eye) of each animal were taken for histopathological analysis. Sections of the mice organs were prepared using the standard histological procedures and analyzed under the light microscope (Axioskop 2 MOT, Carl Zeiss Jena GmbH, Jena, Germany).

Results

Intracellular distribution

After 5 min incubation, ADAP (0.1 and 1 μM) dyed MIAPaCa-2 cell's cytoplasm in red. Sixty minutes later,

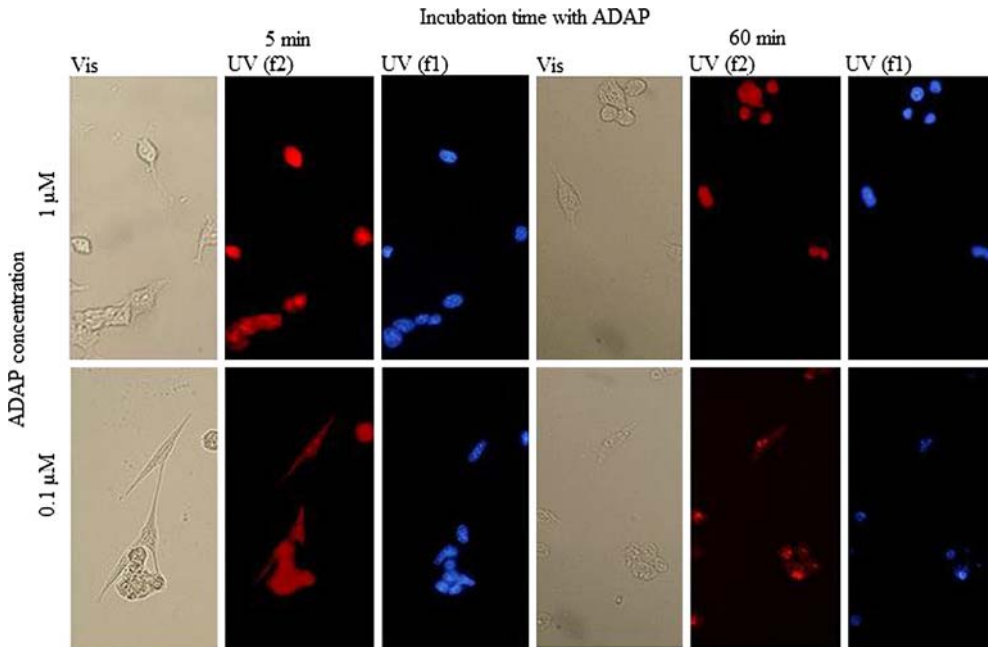

Fig. 2 MIAPaCa-2 cells stained with 0.1 and 1 μM ADAP for 5 and 60 min (UV (f2)), then washed with PBS and stained with 1 nM DAPI for 5 min. DAPI binds selectively to DNA yielding fluorescent nuclei (UV (f1), λ_{max}^{exc} = 340 nm, λ_{max}^{em} = 488 nm). Magnification ×400

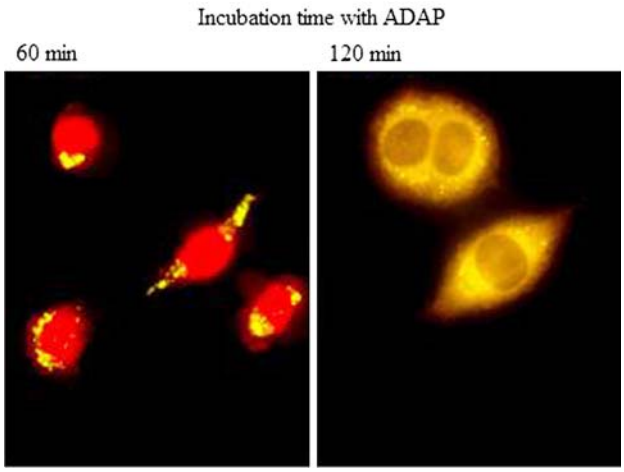

Fig. 3 MIAPaCa-2 cells stained with 10 μM ADAP for 60 and 120 min. Analyzed under UV(f3) filter combination. Magnification ×630

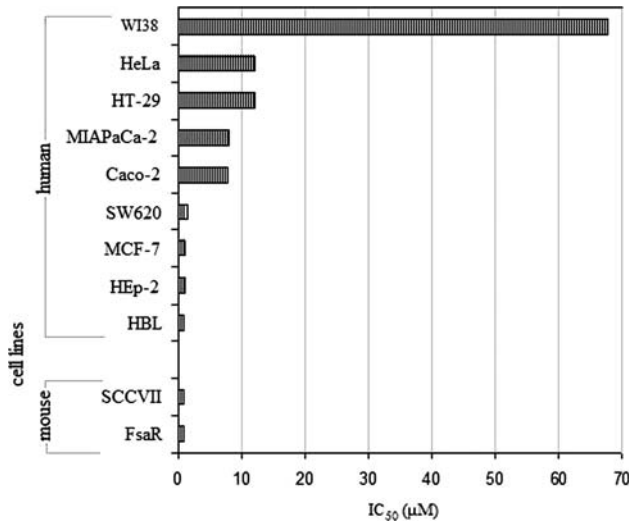

Fig. 4 IC_{50} (μM) of ADAP on various human and mouse cell lines

ADAP was localized preferentially in the cell nuclei. Intracellular accumulation patterns were similar for ADAP and control compound DAPI when MIAPaCa-2 cells were consecutively incubated with these two compounds (Fig. 2). The dependence of uptake and intracellular localization on the concentration of ADAP (0.1 and 1 μM) was not noticed. The 60 min incubation with ADAP (10 μM) caused appearance of a new yellow fluorescence. After the cells were incubated with ADAP for 2 h, red fluorescence disappeared and cells remained yellow (Fig. 3).

Cytotoxic effects

The results of antiproliferative evaluation are expressed as IC_{50} and summarized in Fig. 4. ADAP, in concentrations of 1 and 10 μM, caused strong cytotoxic effects on all treated tumor cells, but did not inhibit the WI38 cell's growth. IC_{50} results show that the concentration of ADAP for 50% growth inhibition of WI38 cells is approximately seven times higher in comparison to HeLa, Caco-2, HT-29 and MIAPaCa-2 cells, and 50–80 times higher in comparison to HBL, HEp-2, SW620 and MCF-7 cells (Fig. 4). Mouse cell

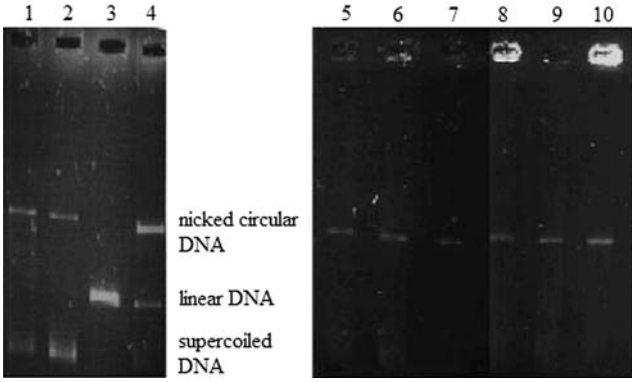

Fig. 5 Effect of ADAP on human topoisomerase IIα-mediated cleavage of pBR322 DNA. Allocation of lanes is as follows: *1* pBR322 plasmid DNA plus human topoisomerase IIα, *2* pBR322 plasmid DNA, *3* as lane *2* plus *Hin*dIII, *4* as lane *2* plus DNaseI, *5–7* as lane *1* plus ADAP (100, 10, 1 μM), *8–10* as lane *1* plus *m*-AMSA (100, 10, 1 μM). Topoisomers originated due to enzymatic activity of human topoisomerase IIα (*1*), linearised plasmid DNA due to *Hin*dIII activity (*3*) and nicked form of plasmid DNA due to action of DnaseI (*4*) are present as controls

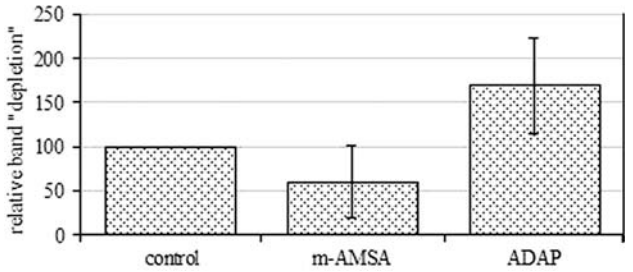

Fig. 6 Results of the immunoband depletion assay of Caco-2 cells treated with ADAP (100 μM, 45 min). Topoisomerase II poison *m*-AMSA was used as a control compound. The intensities of topoisomerase IIα bands were quantified using the ImageQuant^{TL} software and normalized to control band (untreated cells). Results are displayed as averages of two independent experiments ± SD

lines FsaR and SCCVII exibited submicro molar IC_{50} values, similar to human tumor cells HBL.

Effects on human topoisomerase IIα activity

Increasing concentrations of ADAP (1, 10 and 100 μM) did not stimulate the DNA topoisomerase IIα-mediated cleavage (Fig. 5, lanes 5–7) of the pBR322 plasmid DNA. The control DNA intercalator and topisomerase II poison, *m*-AMSA, stimulated DNA topoisomerase IIα-mediated cleavage (Fig. 5, lanes 8–10). Topoisomers originated due to the enzymatic activity of human topoisomerase IIα (Fig. 5, lane 1), linearised plasmid DNA due to *Hin*dIII activity (lane 3) and nicked form of plasmid DNA due to action of DNaseI (lane 4) are present as controls. The reversible complexes between topoisomerase IIα and DNA in the live Caco-2 cells have not been stabilized by 100 μM ADAP (Fig. 6).

Effects on expression of the genes *p53*, *caspase 3*, *c-H-ras, c-N-ras*, *c-Ki-ras* and *c-mos*

ADAP (1 μM) caused the increased expression of *c-Ki-ras*, *c-N-ras*, *c-mos* and *caspase 3* gene products in Caco-2 cells. Transcripts for *c-H-ras* were not detected in treated Caco-2 cells when compared to the control nontreated cells, and the amount of *p53* mRNA in treated cells was similar to that of control cells. The expression of all analyzed genes, except for *c-H-ras* and *p53*, was dependent on the incubation time (3, 12 and 24 h) (Fig. 7).

Effects in vivo

Significant body weight changes of treated animals compared to the controls were not observed, indicating that

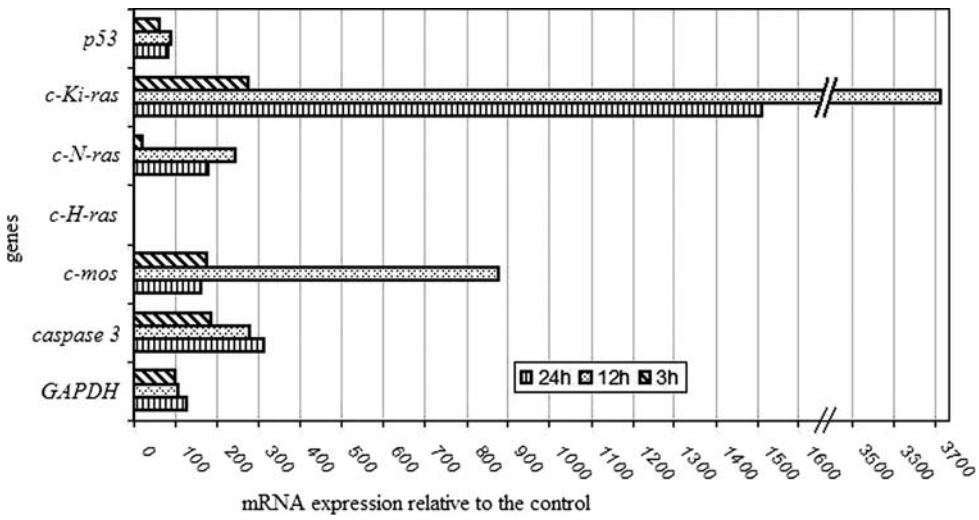

Fig. 7 Expression of the genes *p53*, *c-Ki-ras*, *c-N-ras*, *c-H-ras*, *c-mos*, *caspase 3* and *GAPDH* in treated Caco-2 cells (1 μM ADAP during 3, 12 and 24 h) relative to the control, untreated Caco-2 cells. Expression of the genes in control Caco-2 cells is denoted as a *bold line* denoting 100. The results are representative of two independent experiments

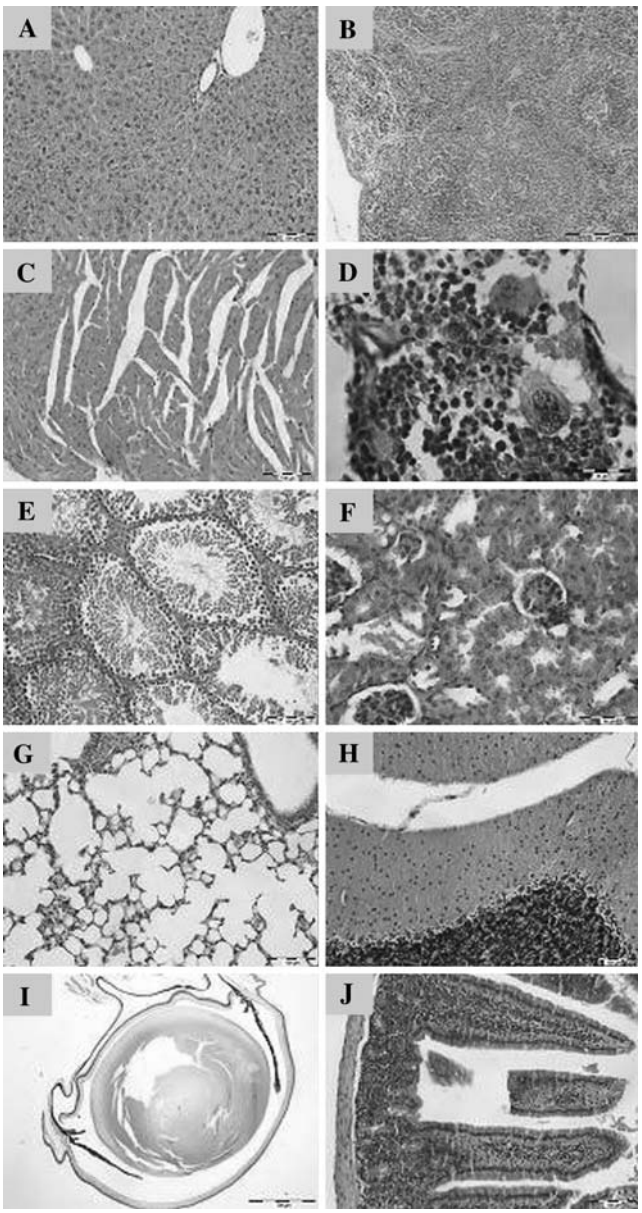

Fig. 8 Sections through the some of the analyzed organs of mouse killed 7th day after single application of ADAP (25 mg/kg). Images on the figure show sections through liver (**a**), spleen (**b**), heart (**c**), bone marrow (**d**), testicle (**e**), renal cortex (**f**), lung (**g**), cerebellar cortex (**h**), eye (**i**), small intestine (**j**)

compound is well tolerated. The highest nonlethal dose (LD_0) of 300 mg/kg was determined after a single injection to mice by i.p. route. In the blood of treated animals killed 7th day after the single application (25 mg/kg), increased concentrations of bilirubin, aspartate aminotransferase (AST), alanine aminotransferase (ALT), lactate dehydrogenase (LDH) and creatinin were found compared to controls. As well as the sections of the organs, especially liver and kidney, of the other experimental groups of mice treated with ADAP and the sections of organs of above-mentioned experimental group did not show morphological changes (Fig. 8). In general, histopathological analysis of sections of the organs of mice treated with single and multiple doses (25 mg/kg) of ADAP, killed at day 7 or 21 after the therapy, showed that there were no morphological changes of tissues and organs, which was confirmed by hematological and clinical-chemical analysis of blood of treated animals (Table 1).

Discussion

Intense red fluorescence of ADAP enabled monitoring of its uptake and distribution in the live cells. Results of our study show that localization of ADAP in the cell is time dependent and independent of tested compound concentration. The mechanism by which ADAP enters into cells is unknown at present but due to its low molecular weight (Mw = 498) and hydrophobic properties well balanced with positive charge, diffusion through cell membrane could be proposed. It is well known that chemical structure of compounds is a key determinant of their uptake and allocation in the live cells [30–32] but is still unknown for positively charged, highly water-soluble drugs [33]. The concentration of ADAP was in close connection to its cytotoxic effects on treated tumor cell lines. Since ADAP has a tendency to intercalate into DNA and RNA [20], assumption was that entry into the cell and formation of complexes with DNA and RNA are the initial steps of cytotoxic activity of ADAP. However, fluorescence microscopy results suggest that within comparatively short period (up to 2 h), ADAP was metabolized into new compound characterized by yellow fluorescence. The previous observation that precursor of ADAP characterized by substituted amino groups in form of amides [20] exhibited yellow fluorescence suggests that in the cell ADAP reacted by forming amide bonds, possibly with some of the peptides. This mode of action would agree nicely with the result presented here that ADAP is not a topoisomerase II poison and therefore its mode of action is not directly related to the interaction with cellular DNA.

The IC_{50} values indicated that the cytotoxicity of ADAP differs distinctively between normal and tumor cell lines, being highly cytotoxic in submicro molar concentration on human melanoma (HBL) cells and mouse fibrosarcoma (FsaR) and squamous carcinoma (SCCVII) cells. Our results showed certain discrepancies in relation to the results of the investigations provided by Yu et al. [21]. The differences were concerned IC_{50} values for ADAP cation on several human cell lines, primarily the WI38 fibroblasts. Our results showed that IC_{50} was 13.5 times higher for WI38 cells, 10 times higher for HT-29 cells and 6 times lower for MCF-7 cells.

Table 1 Effect of ADAP on hematological and clinical-chemical parameters in blood of treated and control mice

Application	ADAP				Control	
	Single		Multiple day 1, 3, 5, 7, 9		–	
Killed day 7 or 21 after the therapy	7	21	7	21	7	21
WBC × 10^9/L	7 ± 1.29	4.6 ± 0.69	6.1 ± 0.89	4.4 ± 0.47	5.9 ± 0.99	4.4 ± 0.17
RBC × 10^{12}/L	7.48 ± 0.72	8.38 ± 0.14	7.43 ± 1.19	8.17 ± 0.41	8.4 ± 0.42	8.39 ± 0.15
HGB g/L	129 ± 7.93	135 ± 1.47	122 ± 15.50	131 ± 4.83	134 ± 5.26	134 ± 2.65
HCT %	0.408 ± 0.04	0.468 ± 0.01	0.402 ± 0.07	0.441 ± 0.02	0.466 ± 0.02	0.453 ± 0.00
MCV fL	54.4 ± 0.91	55.5 ± 1.66	54 ± 0.36	54.2 ± 1.27	55.5 ± 0.30	54.1 ± 0.46
MCH pg	16.7 ± 0.46	16 ± 0.33	16.4 ± 0.71	16.1 ± 0.58	16 ± 0.32	16 ± 0.10
MCHC pg	305 ± 6.35	289 ± 4.58	305 ± 3.61	297 ± 4.85	288 ± 4.36	296 ± 3.21
PLT × 10^9/L	717 ± 481.90	886 ± 173.26	1005 ± 200.59	690 ± 396.92	983 ± 161.53	943 ± 194.28
AST U/L	610 ± 239.16	396 ± 253.76	413 ± 321.05	245 ± 176.82	310 ± 178.88	288 ± 167.66
ALT U/L	101 ± 32.22	83 ± 31.92	60 ± 26.79	64 ± 20.13	68 ± 36.72	70 ± 19.22
AP U/L	111 ± 6.79	164 ± 58.48	141 ± 26.80	114 ± 6.80	146 ± 26.32	135 ± 11.37
LDH U/L	4208 ± 1019.9	3096 ± 1243.7	3188 ± 1807.7	2592 ± 1165.1	3052 ± 623.9	2967 ± 790.3
Glucose mmol/L	5.4 ± 0.84	5.3 ± 1.94	5.2 ± 1.29	5.7 ± 1.07	4.8 ± 1.11	5.4 ± 0.40
Urea mmol/L	12.7 ± 0.97	10.8 ± 3.72	8.7 ± 1.79	9.8 ± 1.38	11.5 ± 1.38	11.9 ± 2.51
Creatinine μmol/L	15 ± 6.43	10 ± 3.27	9 ± 3.20	10 ± 3.78	9 ± 5.09	14 ± 6.08
Bilirubin μmol/L	38 ± 23.44	33 ± 9.29	23 ± 12.16	27 ± 13.72	22 ± 16.27	24 ± 14.57

Results are presented as means ± SD

According to the DNA intercalative characteristics of ADAP observed in isolated system [20], screenings of the topoisomerase II-targeted effects were performed to reveal the possible mechanism of its action. A number of natural and synthetic antitumor drugs have been shown to trap the reversible covalent topoisomerase II–DNA complex converting the topoisomerase II to a DNA damaging agent [15, 34, 35]. Several of these drugs are DNA intercalators [15, 36, 37]. Single stranded and/or double stranded breaks in DNA, which are normally reversible due to action of topoisomerase II, trapped as a result of the action of above-mentioned compounds become permanent lesions and may represent the trigger of apoptosis in cells [15, 34, 35]. Although ADAP binds as an intercalator to isolated DNA and RNA [20], the appearance of single or double stranded breaks, i.e. nicked or linear plasmid form, produced as a result of the action of ADAP was not detected (Fig. 5) suggesting that the mode of action in tumor cells is different from that of DNA intercalation. Furthermore, ADAP did not act as a topoisomerase II poison on the conditions of the experiment (Fig. 6), unlike control DNA intercalating and topoisomerase II poisoning compound *m*-AMSA [38, 39], pointed out that the ADAP's mode of action in tumor cells is different from that of topoisomerase II-poisoning. This is in accordance with our findings of appearance of new yellow fluorescence in cells within 2 h treatment with ADAP. Results of our experiments indicate the possible metabolism of ADAP in the cells within 2 h and generation of a new chemical compound with different fluorescence characteristics. If ADAP chemically reacted by forming amide bond with e.g. peptide, this would certainly result in loss of its DNA intercalative characteristics.

Since it seems that the biological activity of ADAP is not based on its interactions with DNA, we have tried to shed more light on the mechanism pathways by additional studies. As recent findings showed that ADAP caused apoptosis of Caco-2 cells (data not shown), the expression of several genes *p53*, *c-mos*, *c-ras*, *caspase 3* whose protein products take part in apoptosis, has been investigated in Caco-2 cells treated with 1 μM ADAP for 3, 12 and 24 h. Although the role of *c-mos* in cell cycle regulation and apoptosis in somatic cells is not clear yet, there are data indicating the involvement of c-Mos in apoptosis [40] and correlation of its expression with *p53* expression [41, 42]. It has been shown that the expression of wild type *p53* increases as an answer to increased expression of *c-mos* [41], but also that in Caco-2 cells one allele of the *p53* gene is mutated (stop codon at position 204 of codon 6) and the other allele is deleted [43]. However, different mutations in *p53* gene are not functionally equivalent [44]. In this study, the expression of *p53* has been slightly decreased compared to control and correlation between *p53* and *c-mos* expression has not been detected. Results of the role of *c-ras* oncogenes in promotion [45–48] and/or suppression of apoptosis [49, 50] are contradictory. Presence of procaspase 3 in cells is one of the factors that affect the

readiness for apoptosis [51] and its synthesis de novo could be an indicator of triggered apoptosis in treated tumor cells. The expression of *c-Ki-ras*, *c-N-ras*, *c-mos* and *caspase 3* transcripts has been increased due to action of ADAP and is dependent on the incubation time (Fig. 7), which pointed out the possible role of these genes in apoptotic cell death of treated Caco-2 cells.

Mice treated with ADAP and control mice were killed, and their tissue and blood samples were taken at day 7 and 21 after the therapy because the tissue damage usually appears within few days to few weeks after the application of chemical compound. Moderately increased activity of aspartate aminotransferase (AST), alanine aminotransferase (ALT) and lactate dehydrogenase (LDH) in the serum of the mice killed at day 7 after the single application (25 mg/kg) of ADAP (Table 1) suggested appearance of lesions or changes in membrane permeability of hepatocytes. But decrease and normalization of the activity of these enzymes, 3 weeks after the single application of ADAP (Table 1) pointed out that hepatocyte damage was transient, which has been confirmed by patohistological analysis of the liver sections (Fig. 7) of mice. Increased concentrations of bilirubin and creatinine in the serum of the same experimantal group of animals (single application od ADAP, killed at day 7) were transient and without effect on the morphology of the examined organs (Fig. 7). There was no activity of γ-glutamyl transferase in the blood of mice of the treated and control experimental groups, which showed that single and multiple applications of 25 mg/kg of ADAP did not cause liver damage in treated mice. Number of red blood cells (RBC), white blood cells (WBC) and platelets (PLT), concentration of hemoglobin (HGB), mean corpuscular volume (MCV), mean corpuscular hemoglobin (MCH) and mean corpuscular hemoglobin concentration (MCHC) did not considerably differ in the blood of mice treated with ADAP in relation to control mice (Table 1). The values of all measured hematological parameters were typical for mice [52].

Conclusion

We can conclude that the chemical structure of ADAP does not represent barrier for its uptake into live cells and its distribution inside the cells is time dependent. Besides, concentration of ADAP does not affect its intracellular uptake and localization. ADAP has a strong antitumor activity in vitro nevertheless it is not toxic in vivo, on mice. Although ADAP is a DNA and RNA intercalator, its mode of action in cancer cells could be different than DNA intercalation as well as different than topoisomerase II poisoning. This is in accordance with our findings of possible metabolizing of ADAP in the cells into new chemical compound with different fluorescence properties, possibly chemically bound over amide bonds to a peptide. Time dependent changes in expression of *c-Ki-ras*, *c-N-ras*, *c-mos* and *caspase 3* transcripts suggest the possible role of these genes in apoptosis triggered by action of ADAP. Based on ADAP's strong antitumor potential in vitro and due to absence of its toxic effects on mice, we intend to examine antitumor activity of ADAP in vivo.

Acknowledgments This project was supported by the Ministry of Science, Education and Sport, Republic of Croatia, grants 0127111 and 219-0982914-2176. We are grateful to Prof. Dr. Mirjana Knežević-Kostović and M.Sc. Neda Cetina for their kind support.

References

1. Ferlay J, Parkin MD, Pisani P (1998) Globocan: Cancer incidence and mortality worldwide. International Agency for Research on Cancer, IARC Cancer Base, Lyon, France, pp 3
2. Howard CV, Newby JA (2004) Could the increase in cancer incidence be related to recent environmental changes. In: Nicolopoulou-Stamati P, Hens L, Howard CV, Van Larebeke L (eds) Cancer as an environmental disease. Kluwer, Dordrecht
3. Li Q, Xu W (2005) Novel anticancer targets in drug discovery in postgenomic age. Curr Med Chem Anticancer Agents 5:53–63
4. Lerman LS (1961) Structural considerations in the interaction of DNA and acridines. J Mol Biol 3:18–30
5. Demeunyck M, Bailly C, Wilson WD (2002) DNA and RNA binders: from small molecules to drugs. Wiley, New York
6. Silverman RB (2004) The organic chemistry of drug design and drug action, 2nd edn. Elsevier, San Diego
7. Taylor IW, Milthorpe BK (1980) An evaluation of DNA fluorochromes, staining techiques and analysis for flow cytometry. J Histochem Cytochem 28(11):1224–1232
8. Benson SC, Mathies RA, Glazer AN (1993) Heterodimeric DNA-binding dyes designed for energy transfer: stability and applications of the DNA complexes. Nucleic Acids Res 21(24):5720–5726
9. Biver T, De Biasi A, Secco F, Venturini M, Yarmoluk S (2005) Cyanine dyes as intercalating agents: kinetic and thermodinamic studies on the DNA/Cyan40 and DNA/CCyan2 systems. Biophys J 89:374–383
10. Yang XL, Wang AH-J (1999) Structural studies of atom-specific drugs on DNA. Pharmacol Ther 83:181–215
11. Brańa MF, Cacho M, Gradillas A, Pascual-Teresa B, Ramos A (2001) Intercalators as anticancer drugs. Curr Pharm Des 7:1745–1780
12. Martinez R, Chacon-Garcia L (2005) The search of DNA-intercalators as antitumoral drugs: what it worked and what did not work. Curr Med Chem 12(2):127–151
13. Subramanian D, Sommer FC, Muller MT (2001) ICE Bioassay. In: Osheroff N, Bjornsti M-A (eds) DNA Topoisomerase protocols. Enzymology and drugs. Humana Press, Totowa, pp 137–147
14. Ehlert JE, Kubbutat MHG (2001) Apoptosis and its relevance in cancer therapy. Onkologie 24:433–440
15. Hurley LH (2002) DNA and its associated processes as targets for cancer therapy. Nat Rev Cancer 2:188–200
16. Akimitsu N, Kamura K, Toné S, Sakaguchi A, Kikuchi A, Hamamoto H, Sekimizu K (2003) Induction of apoptosis by depletion of topoisomerase II in mammalian cells. Biochem Biophys Res Commun 307:301–307

17. Kaina B (2003) DNA damage-triggered apoptosis: critical role of DNA repair, double-strand breaks, cell proliferation and signaling. Biochem Pharmacol 66:1547–1554
18. Palm BS, Piantanida I, Žinić M, Schneider H-J (2000) The interaction of new 4,9-diazapyrenium compounds with double stranded nucleic acids. J Chem Soc – Perkin Trans II:385–392
19. Piantanida I, Tomšić V, Žinić M (2000) 4,9-Diazapyrenium cations. Synthesis, physico-chemical properties and binding of nucleotides in water. J Chem Soc Perkin Trans II:375–383
20. Piantanida I, Palm BS, Žinić M, Schneider H-J (2001) A new 4,9-diazapyrenium intercalator for single- and double-stranded nucleic acids: distinct differences from related diazapyrenium compounds and ethidium bromide. J Chem Soc Perkin Trans II(9):1808–1816
21. Yu D-H, MacDonald J, Josephs S, Liu Q, Nguy V, Tor Y, Wong-Staal F, Li Q-X (2006) MDDD, a 4,9-diazapyrenium derivative, is selectively toxic to glioma cells by inducing growth arrest at G0/G1 independently of p53. Invest New Drugs 24:489–498
22. Steiner-Biočić I, Glavaš-Obrovac L, Karner I, Piantanida I, Žinić M, Pavelić K, Pavelić J (1996) 4,9-Diazapyrenium dications induce apoptosis in human tumor cells. Anticancer Res 16:3705–3708
23. Roknić S, Glavaš-Obrovac L, Karner I, Piantanida I, Žinić M, Pavelić K (2000) In vitro cytotoxicity of three 4,9-diazapyrenium hydrogensulfate derivatives on different human tumor cell lines. Chemotherapy 46:143–149
24. Marczi S, Glavaš-Obrovac L, Karner I (2005) Induction of apoptosis of human tumor cells by a 4,9-diazapyrenium derivative and its effects on topoisomerase-II action. Chemotherapy 51:217–222
25. Piantanida I, Žinić M, Marczi S, Glavaš-Obrovac L (2007) Bis-4,9-diazapyrenium dications: synthesis of the methylenedibenzyl-analogue, interactions with nucleotides, DNA, RNA. The antitumor activity of all till now prepared analogues. J Phys Org Chem 20:285–295
26. Mickisch G, Fajta S, Keilhauer G, Schlick E, Tschada R, Alken P (1990) Chemosensitivity testing of primary human renal cell carcinoma by a tetrazolium based microculture assay (MTT). Urol Res 18:131–136
27. Burden DA, Froelich-Ammon J, Osheroff N (2001) Topoisomerase I-mediated cleavage of plasmid DNA. In: Osheroff N, Bjornsti M-A (eds) DNA topoisomerase protocols. Enzymology and drugs. Humana Press Inc., New Yersey, pp 283–289
28. Kaufmann SH, Svingen PA (2001) Immunoblot analysis and bend depletion assay. In: Bjornsti M-A, Osheroff N (eds), DNA topoisomerase protocols. DNA topology and enzymes. Humana Press Inc., New Yersey, pp 253–268
29. Laemmli UK (1970) Cleavage of structural proteins during the assembly of head of bacteriophage T4. Nature 227:680–685
30. Gedda L, Silvander M, Sjöberg S, Tjarks W, Carlsson J (1997) Cytotoxicity and subcellular localization of boronated phenanthridinium analogues. Anticancer Drug Des 12:671–685
31. Haldane A, Finlay GJ, Hay MP, Denny WA, Baguley BC (1999) Cellular uptake of N-[2-(dimethylamino)ethyl]acridine-4-carboxamide (DACA). Anticancer Drug Des 14:275–280
32. Hicks KO, Pruijn FB, Baguley BC, Wilson WR (2001) Extravascular transport of the DNA intercalator and topoisomerase poison N-[2-(dimethylamino)ethyl]acridine-4-carboxamide (DACA): diffusion and metabolism in multicellular layers of tumor cells. J Pharmacol Exp Ther 297:1088–1098
33. Lansiaux A, Dassonneville L, Facompré M, Kumar A, Stephens CE, Bajic M, Tanious F, Wilson WD, Boykin DW, Bailly C (2002) Distribution of furamidine analogues in tumor cells: influence of the number of positive charges. J Med Chem 45:1994–2002
34. Cline S, Osheroff N (1999) Cytosine arabinoside lesions are position-specific topoisomerase II poisons and stimulate DNA cleavage mediated by the human type II enzymes. J Biol Chem 274:29740–29743
35. Rowe TC, Grabowski D, Ganapathi R (2001) Isolation of covalent enzyme-DNA complexes. In: Osheroff N, Bjornsti M-A (eds) DNA topoisomerase protocols. Enzymology and drugs. Humana Press Inc, New Jersey, pp 129–136
36. Kim SG, Sung M, Kang KW, Kim SH, Son MH, Kim WB (2001) DA-125, a novel anthracycline derivative showing high-affinity DNA binding and topoisomerase II inhibitory activities, exerts cytotoxicity via c-Jun N-terminal kinase pathway. Cancer Chemother Pharmacol 47:511–518
37. Bal C, Baldeyrou B, Moz F, Lansiaux A, Colson P, Kraus-Berthier L, Leonce S, Pierre A, Boussard M-F, Rousseau A, Wierzbicki M, Bailly C (2004) Novel antitumor indenoindole derivatives targeting DNA and topoisomerase II. Biochem Pharmacol 68:1911–1922
38. Marsh KL, Willmore E, Tinelli S, Cornarotti M, Mectes EL, Capranico G, Fisher LM, Austin CA (1996) Amsacrine-promoted DNA cleavage site determinants for the two human DNA topoisomerase II isoforms alpha and beta. Biochem Pharmacol 52:1675–1685
39. Finlay GJ, Atwell GJ, Baguley BC (1999) Inhibition of the action of the topoisomerase II poison amsacrine by simple aniline derivatives: evidence for drug-protein interactions. Oncol Res 11(6):249–254
40. Yew N, Strobel M, Vande Woude GF (1993) Mos and the cell cycle: the molecular basis of the transformed phenotype. Curr Opin Genet Dev 3(1):19–25
41. Fukasawa K, Vande Woude GF (1997) Synergy between the Mos/mitogen-activated protein kinase pathway and loss of p53 function in transformation and chromosome instability. Mol Cell Biol 17(1):506–518
42. Lyons SK, Clarke AR (1997) Apoptosis and carcinogenesiy. Br Medical Bull 53:554–569
43. Djelloul S, Forgue-Lafitte M-E, Hermelin B, Mareel M, Bruyneel E, Baldi A, Giordano A, Chastre E, Gespach C (1997) Enterocyte differentiation is compatible with SV40 large T expression and loss of p53 function in human colonic Caco-2 cells. FEBS Lett 406:234–242
44. Pietsch EC, Humbey O, Murphy ME (2006) Polymorphisms in the p53 pathway. Oncogene 25:1602–1611
45. Thompson CB (1995) Apoptosis in the pathogenesis and treatment of disease. Science 267:1456–1462
46. Mayo MW, Wang CY, Cogswell PC, Rogers-Graham KS, Lowe SW, Der CJ, Baldwin AS Jr (1997) Requirement of NF-κB activation to suppress p53-independent apoptosis induced by oncogenic Ras. Science 278:1812–1815
47. Shapiro P (2001) Ras-MAP kinase signaling pathways and control of cell proliferation: relevance to cancer therapy. Crit Rev Clin Lab Sci 39(4–5):285–330
48. Moon A (2006) Differential functions of Ras for malignant phenotypic conversion. Arch Pharm Res 29(2):113–122
49. Ward RL, Todd AV, Santiago F, O'Connor T, Hawkins NJ (1997) Activation of the K-ras oncogene in colorectal neoplasms is associated with decreased apoptosis. Cancer 79(6):1106–1113
50. Downward J (1998) ras signaling and apoptosis. Curr Opin Genet Dev 8:49–54
51. Bowen C, Voeller HJ, Kikly K, Gelmann EP (1999) Synthesis of procaspase-3 and -7 during apoptosis in prostate cancer cells. Cell Death Differ 6:394–401
52. Moore DM (2000) Hematology of the mouse. In: Feldman BV, Zinkl JG, Jain NC (eds) Schalm's veterinary hematology. Lippincot Williams & Wilkons, Philadelphia, pp 1219–1224